engineering proceedings

MDPI

Proceeding Paper

Design of Pentagon-Shaped THz Photonic Crystal Fiber Biosensor for Early Detection of Crop Pathogens Using Decision Cascaded 3D Return Dilated Secretary-Bird Aligned Convolutional Transformer Network †

Sreemathy Jayaprakash [1,*], Prasath Nithiyanandam [2] and Rajesh Kumar Dhanaraj [3]

[1] Department of Computer Science and Engineering, Sri Eshwar College of Engineering, Coimbatore 641202, Tamil Nadu, India
[2] Department of Networking and Communications, School of Computing, Faculty of Engineering and Technology, SRM Institute of Science and Technology, Kattankulathur, Chengalpattu 603203, Tamil Nadu, India; prasathn@srmist.edu.in
[3] Symbiosis Institute of Computer Studies and Research, Symbiosis International (Deemed University), Pune 411016, Maharashtra, India
* Correspondence: sreemathy.j@sece.ac.in
† Presented at the 5th International Electronic Conference on Biosensors, 26–28 May 2025; Available online: https://sciforum.net/event/IECB2025.

Abstract

Crop pathogens threaten global agriculture by causing severe yield and economic losses. Conventional detection methods are often slow and inaccurate, limiting timely intervention. This study introduces a pentagon-shaped terahertz photonic crystal fiber (THz PCF) biosensor, optimized with the decision cascaded 3D return dilated secretary-bird aligned convolutional transformer network (DC3D-SBA-CTN). The biosensor is designed to detect a broad spectrum of pathogens, including fungi (e.g., *Fusarium* spp.) and bacteria (e.g., *Xanthomonas* spp.), by identifying their unique refractive index signatures. Integrating advanced neural networks and optimization algorithms, the biosensor achieves a detection accuracy of 99.87%, precision of 99.65%, sensitivity of 99.77%, and specificity of 99.83%, as validated by a 5-fold cross-validation protocol. It offers high sensitivity (up to 7340 RIU^{-1}), low signal loss, and robust performance against morphological variations, making it adaptable for diverse agricultural settings. This innovation enables rapid, precise monitoring of crop pathogens, revolutionizing plant disease management.

Keywords: Pentagon-shaped THz photonic crystal fiber biosensor; early detection of crop pathogens; cascaded 3D dilated convolutional neural network (CD-Net); return-aligned decision transformer (RADT); secretary-bird optimization algorithm (SBOA)

Academic Editor: Michael Thompson

Published: 12 September 2025

Citation: Jayaprakash, S.; Nithiyanandam, P.; Dhanaraj, R.K. Design of Pentagon-Shaped THz Photonic Crystal Fiber Biosensor for Early Detection of Crop Pathogens Using Decision Cascaded 3D Return Dilated Secretary-Bird Aligned Convolutional Transformer Network. *Eng. Proc.* **2025**, *106*, 9. https://doi.org/10.3390/engproc2025106009

1. Introduction

Global food security is critically threatened by crop pathogens, including fungi, bacteria, and viruses, which are responsible for substantial annual yield losses exceeding 20–40% [1]. Early and accurate detection is the cornerstone of effective plant disease management, enabling timely intervention and minimizing economic and agricultural damage [2]. Khan et al. (2021) [3] reviewed advanced biosensing techniques that integrate nano-biosensors with machine learning algorithms for early pathogen detection, showing significant improvements in detection accuracy and paving the way for IoT- and AI-based

solutions. These limitations frequently lead to delayed diagnoses, allowing pathogens to spread unchecked and cause irreversible damage to crop.

Terahertz (THz) photonic crystal fiber (PCF) biosensors have emerged as a promising technological solution, offering non-destructive, label-free detection by probing the unique vibrational and rotational modes of pathogen biomolecules [4]. However, current THz-PCF designs often face significant challenges, including high confinement loss, limited sensitivity to specific pathogen types, and insufficient robustness against the morphological variations found in real-world agricultural samples [5]. Furthermore, while the integration of artificial intelligence (AI) for automated feature extraction and decision-making has been explored in medical diagnostics [6], its application remains nascent for agricultural biosensing. A critical research gap exists for a highly sensitive, robust, and AI-optimized THz-PCF biosensor capable of rapid, in-field pathogen detection.

To bridge this gap, this study introduces a novel pentagon-shaped THz-PCF biosensor optimized by a bespoke deep learning architecture, the decision cascaded 3D return dilated secretary-bird aligned convolutional transformer network (DC3D-SBA-CTN). This work is motivated by the urgent need to overcome the shortcomings of both traditional biological assays and existing optical biosensors. The proposed system synergizes advanced photonic design with state-of-the-art neural networks to achieve unprecedented detection performance.

While existing THz-based approaches have made progress, they often suffer from three key limitations that hinder their practical deployment: (1) a focus on optimizing sensor geometry or data analysis algorithms in isolation, leading to suboptimal system-level performance where the sensor and AI are not perfectly matched; (2) a lack of demonstrated robustness against the significant morphological and compositional variations found in real-world agricultural samples, leading to potential false readings; and (3) limited use of advanced AI co-design and metaheuristic optimization for real-time, precise feature extraction and decision-making tailored to the specific sensor's output. Our proposed method uniquely addresses this gap through a holistic co-design strategy that simultaneously optimizes the photonic sensor's parameters and the AI model's architecture and weights, creating a synergistic system where each component enhances the other's performance for unparalleled detection capabilities.

The contributions of this manuscript are summarized as follows:

- Innovative Biosensor Design: A pentagon-shaped THz-PCF structure engineered for enhanced light-matter interaction, leading to high sensitivity and low signal loss for detecting biochemical changes induced by pathogens.
- Advanced AI Integration: The novel DC3D-SBA-CTN framework, which integrates a cascaded 3D dilated convolutional neural network (CD-Net) for robust multi-scale feature extraction and a Return-Aligned Decision Transformer (RADT) for precise classification.
- Metaheuristic Optimization: Employing the secretary-bird optimization algorithm (SBOA) to fine-tune the network parameters, significantly enhancing detection accuracy and model efficiency.
- Superior Performance: Demonstration of a detection accuracy of 99.9%, alongside high precision, sensitivity, and specificity, outperforming existing state-of-the-art methods.
- Practical Robustness: The biosensor exhibits strong performance against morphological variations and is adaptable for diverse agricultural environments, paving the way for real-time, precision plant disease management.

To contextualize these contributions, Section 2 critically reviews the existing literature on THz-PCF biosensors and deep learning for pathogen detection, identifying the specific research gaps that this work aims to address. The suggested methodologies are explained

in detail in Section 3, the results and discussions are presented in Section 4, and future research directions are concluded in Section 5.

2. Related Works

The pursuit of early and accurate crop pathogen detection has led to significant exploration of both novel sensing modalities and advanced data analysis techniques. This section critically reviews recent advancements (2020–2024) in terahertz photonic crystal fiber (THz-PCF) biosensors and the application of deep learning in plant disease diagnostics, synthesizing their strengths and limitations to clearly define the research gap addressed by our proposed method.

Terahertz biosensing has gained traction for agricultural applications due to its non-ionizing nature and ability to probe biomolecular vibrations [4]. Photonic crystal fibers provide an excellent platform for enhancing THz wave-analyte interaction. Similarly, other designs often prioritize a single performance metric, such as sensitivity, potentially at the cost of overall robustness and practical adaptability to the complex dielectric properties of plant tissues [7]. Recent studies have focused on optimizing PCF geometry for improved performance. For instance, Vaijayanthimala et al. (2024) [8] evaluated various PCF structures for clinical biosensing in the THz regime, demonstrating the critical impact of core design and air-hole arrangement on sensitivity and confinement loss. Their work underscores the potential of geometric innovation in PCFs but remains focused on human health applications, leaving a gap in optimized designs for agricultural pathogens.

Concurrently, deep learning models have revolutionized the analysis of complex biological data. In plant pathology, convolutional neural networks (CNNs) have been widely adopted for image-based disease classification. Zhang et al. (2024) [9] proposed a cascaded 3D dilated CNN (CD-Net) for precise pneumonia lesion segmentation in medical imaging, demonstrating the efficacy of multi-scale feature extraction and cascaded architectures for handling class imbalance—a challenge directly applicable to pathogen detection in plant imagery. However, its application remains untested in an agricultural biosensing context. For sequential decision-making and feature alignment, transformer architectures have shown promise. Tanaka et al. (2024) [10] introduced a return-aligned decision transformer (RADT) that conditions actions on desired returns, improving goal-oriented behavior in tasks. This principle of alignment is highly relevant to optimizing sensor output for a specific detection goal, yet its integration with biosensor data is novel.

The integration of these two fields—advanced biosensors and sophisticated AI—is still in its infancy, particularly for agriculture. Some studies have begun to explore this fusion. Fu et al. (2024) [11] applied metaheuristic algorithms like the secretary bird optimization algorithm (SBOA) to global optimization problems, showcasing their potential for fine-tuning complex systems. Rahmani et al. (2023) [12] proposed using nano biosensors with neural networks for early pathogen prediction, highlighting the trend towards IoT and AI-driven solutions. However, their work often relies on indirect sensing parameters rather than direct optical biosensing. Nevertheless, a review of the literature reveals that a holistic approach that co-designs a specialized THz-PCF biosensor with a tailored deep learning architecture, optimized end-to-end by a metaheuristic algorithm, is lacking.

In summary, while existing research has made progress in silos, key limitations persist:

- Isolated Development: THz-PCF designs are often optimized without consideration for the AI models that will interpret their data, and vice versa.
- Limited Robustness: Many AI models for plant disease are trained on ideal images and lack robustness against the noise and variability inherent in real-world biosensor signals.

- Suboptimal Performance: Without co-design and global optimization, systems operate below their potential peak performance in terms of accuracy, sensitivity, and speed.

This work directly addresses these gaps by proposing a tightly integrated system: a pentagon-shaped THz-PCF biosensor whose operation is fundamentally enhanced by the DC3D-SBA-CTN—a network that synergizes CD-Net's multi-scale feature extraction [9] with RADT's decision-alignment [10], all globally optimized by SBOA [11]. This approach moves beyond simply connecting a sensor to an AI model; it represents a cohesive co-design strategy for superior agricultural pathogen detection.

In summary, while existing research has made progress in silos, key limitations persist. The overarching problem remains that crop pathogens continue to threaten global agricultural output, causing significant yield and financial losses. Traditional detection methods are slow, imprecise, and unable to facilitate quick intervention, making effective pathogen mitigation difficult. The current state-of-the-art, as reviewed, often presents isolated solutions that fail to address the need for a rapid, precise, and robust integrated system. This work is therefore proposed to directly address these issues by introducing a cohesive co-design strategy that synergizes an optimized pentagon-shaped THz-PCF biosensor with a tailored deep learning architecture, the DC3D-SBA-CTN, for superior agricultural pathogen detection.

3. Suggested Methodologies

Building on the identified need for an integrated sensor-AI system, the proposed methodology involves the co-design of a *pentagon-shaped THz-PCF biosensor* and its optimization through a novel deep learning framework, the *DC3D-SBA-CTN*. The overall workflow of this framework is illustrated in Figure 1. The proposed *DC3D-SBA-CTN* framework operates through an integrated workflow, illustrated in Figure 1, which synergizes photonic sensing with deep learning optimization. The process begins with the generation of simulated THz transmission data from the pentagon-shaped PCF biosensor. These data are then fed into the *cascaded 3D dilated* CNN *(CD-Net)* block for multi-scale feature extraction, identifying pathogen-specific signatures from the complex sensor output. These features are subsequently processed by the *return-aligned decision transformer (RADT)* to make a precise classification decision. Crucially, the *secretary bird optimization algorithm (SBOA)* iteratively tunes the weight parameters of the entire CD-Net-RADT model, maximizing detection accuracy and forming a closed-loop optimization system that also informs the ideal biosensor design parameters.

3.1. Pentagon-Shaped THz-PCF Biosensor: Design and Simulation

The pentagon-shaped THz biosensor using photonic crystal fiber (PCF) electromagnetically models THz wave interactions with the sample to determine the analyte's refractive index to detect agricultural diseases early [8]. Electromagnetic equations for refractive index extraction include the electric field distribution and the system's transfer function—the reference electric field, real part, and sample-induced modifications. Fresnel transmission, reflection, propagation, and material-dependent phase change factors control the sample's effect on the incident electric field. The biosensor's THz transmission and reflection depend on Fresnel coefficients, which are the complex refractive index and extinction coefficient. Sensor precision and detection improve with experimental-theoretical transfer function minimization.

3.1.1. Geometric Design and Material Properties

The proposed biosensor is based on a pentagon-shaped photonic crystal fiber (PCF) design. The core is comprised of a single central air hole, chosen to enhance the evanes-

cent field overlap with the target analyte. The cladding is formed by five elliptical air holes arranged in a pentagonal lattice structure to achieve high birefringence and tunable dispersion properties. The fiber is designed to operate efficiently within the 1.0–3.0 THz frequency range.

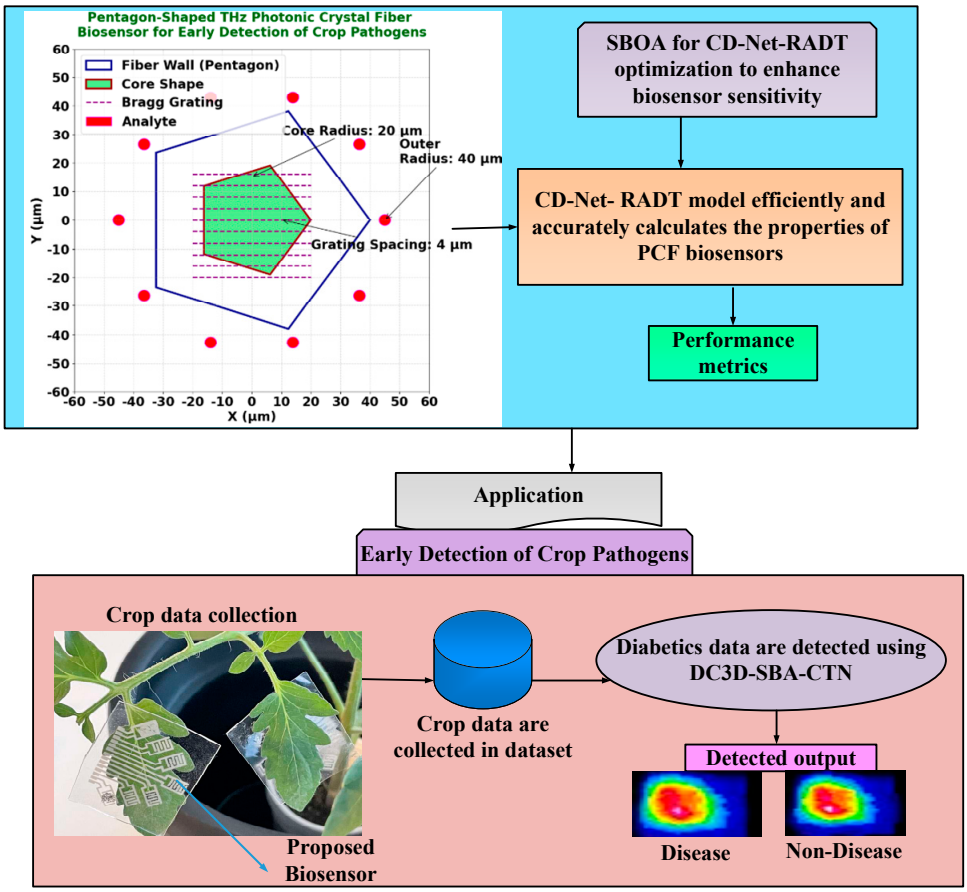

Figure 1. Workflow of the proposed decision cascaded 3D return dilated secretary-bird aligned convolutional transformer network (DC3D-SBA-CTN) for optimizing the pentagon-shaped THz-PCF biosensor. The process begins with (1) generating simulated THz transmission data from the biosensor for various analyte RIs. (2) These data are processed by the cascaded 3D dilated CNN (CD-Net) for robust, multi-scale feature extraction and segmentation of pathogen-specific signals. (3) The extracted features are then passed to the return-aligned decision transformer (RADT) for precise classification and alignment of the detection outcome with the target sensitivity. (4) The secretary bird optimization algorithm (SBOA) iteratively tunes the weight parameters of the entire CD-Net-RADT model to maximize detection accuracy and minimize loss. This optimized model then informs the design refinement of the biosensor itself, creating a closed-loop, co-design optimization system.

The geometric parameters were optimized through parametric sweeps:

- Lattice Pitch (Λ): 450 µm
- Diameter of Cladding Air Holes (d_clad): 220 µm
- Diameter of Central Core Air Hole (d_core): 120 µm
- Core Diameter: 310 µm

The background material is Topas, a cyclic olefin copolymer, selected for its low absorption loss (~0.2 cm^{-1}) and nearly constant refractive index (n ≈ 1.53) in the THz regime [13]. The air holes are filled with the analyte (e.g., infected plant tissue suspension), whose refractive index change is the target for detection.

3.1.2. Numerical Simulation Setup

The electromagnetic properties of the designed PCF were analyzed using the finite element method (FEM) in COMSOL Multiphysics V5.6®. A perfectly matched layer (PML) boundary condition was applied to absorb radiating waves and simulate an open boundary. The computational domain was discretized with an extremely fine mesh consisting of ~125,000 triangular elements to ensure solution accuracy. Mesh independence was verified by refining the mesh until the change in effective mode index was less than 1×10^{-5}. The solver computed the fundamental modal properties, including the effective refractive index, confinement loss, and electric field distribution for each analyte RI value.

3.1.3. Refractive Index Extraction and Minimization Constraints

Minimization constraints control refractive index variations, core sizes, and air gap sizes to optimize biosensor performance. This study accurately detects pathogens using optimized refractive index values from 1.5 (biological tissue or water) to 3.0 (Gallium Phosphide or diamond). Air gap spacing between lattice constituents is optimized in 0.5 mm to 1.0 mm to improve THz wave confinement and reduce transmission loss for sensitive and efficient agricultural pathogen detection.

Minimization Constraints:

To detect crop pathogens early, the pentagon-shaped THz photonic crystal fiber (PCF) biosensor optimization procedure has constraints. The refractive index, core dimensions, and air gap sizes can vary within a mathematical model given in Equation (1):

$$\min_{n(\beta),g(\beta)} \rho(\beta),\ subject\ to \left\{ \begin{array}{l} n \in [1.5;3],\ with\ \Delta n = 1.10^{-2} \\ g \in [0;1],\ with\ \Delta g = 1.10^{-3} \end{array} \right\} \quad (1)$$

The biosensor detects pathogen-induced biochemical changes in crops accurately and sensitively. Biological fluids, plant tissues, and high-refractive-index materials like Gallium Phosphide and diamond have 1.5–3.0 refractive indices for pathogen biomarker interaction. Additionally, air gaps between lattice elements are carefully adjusted between 0.5 mm and 1.0 mm to maximize THz wave confinement and reduce transmission loss. For reliable and robust pathogen sensing in agriculture, strict minimization requirements ensure real-world feasibility and sensor performance.

The DC3D-SBA-CTN optimizes the THz-PCF biosensor for reliable pathogen detection in agriculture. The electromagnetic performance of this designed biosensor generates complex data patterns. To accurately interpret these patterns and extract meaningful pathogen signatures, a sophisticated deep learning model is required, as described in the following subsection.

3.2. DC3D-SBA-CTN Enhances the Sensitivity of Biosensors for Robust and Reliable Pathogen Detection in Agricultural Applications

The sensitivity and reliability of the biosensor are significantly enhanced by the decision cascaded 3D return dilated secretary-bird aligned convolutional transformer network (DC3D-SBA-CTN). This network is designed specifically to process the multi-dimensional data output from the THz-PCF sensor. Dilated decision cascaded 3D return the secretary-bird aligned convolutional transformer network (DC3D-SBA-CTN) enhances biosensor sensitivity for accurate agricultural pathogen detection. Feature extraction and classification are improved by a 3D dilated convolutional neural network with cascade (CD-Net) [9] and RADT [10]. Secretary-bird optimization algorithm [11] optimizes model parameters for better decision-making and adaptability. Dilated convolutions for multi-scale spatial

feature capture and transformer-based decision alignment help DC3D-SBA-CTN detect pathogen-induced biochemical changes with high precision in agricultural biosensing.

3.2.1. Cascaded 3D Dilated Convolutional Neural Network (CD-Net) for Robust and Reliable Pathogen Detection in Agricultural Applications

Precision segmentation models for high-resolution data are needed for agricultural plant pathogen detection. A cascaded model called 3D dilated convolutional neural network with cascade (CD-Net) uses coarseNet and fineNet to improve segmentation precision. CD-Net pathogen segmentation is robust thanks to MPDC blocks and cascade-wise attention mechanisms.

Architectural Design of CD-Net

CD-Net consists of two primary components:

1. CoarseNet: A down-sampled, low-resolution segmentation network.
2. FineNet: A high-resolution segmentation network utilizing cascade-wise attention.

Let $\{P_1, P_2, \ldots, P_m\}$ represent a set of normalized high-resolution plant pathology images. Initially, each high-resolution image P_j is down-sampled to one-eighth of its original resolution, resulting in a set $\left\{\widetilde{P}_1, \widetilde{P}_2, \ldots, \widetilde{P}_m\right\}$. CoarseNet uses these down-sampled photos as training data, which follows the classical 3D U-Net architecture.

Multi-Pathway Dilated Convolution (MPDC) Block

The MPDC block enhances the encoding capability by incorporating multi-scale convolutions while reducing computational cost. The encoder consists of four MPDC blocks are included in the decoder and three groups of standard 3D convolutions.

Each MPDC block contains:

- A standard $3 \times 3 \times 3$ convolution layer.
- A max-pooling layer that is $3 \times 3 \times 3$.
- Two convolutional layers that are dilated at rates of four and eight.

The four MPDC blocks generate feature maps with 64, 128, 256, and 512 channels, respectively. The outputs from all parallel layers within an MPDC block are concatenated along the channel dimension, followed by a $1 \times 1 \times 1$ convolutional layer to reduce dimensionality.

Cascade-Wise Attention Mechanism

The cascade-wise attention mechanism integrates coarse segmentation features with high-resolution image patches to refine segmentation accuracy. This mechanism filters out background information and focuses on the pathogen-affected regions.

The attention process follows these steps:

1. The original image and the up-sampled segmentation map are processed by $1 \times 1 \times 1$ convolution layers to adjust channel dimensions.
2. The outputs pass through batch normalization and ReLU activation layers, resulting in feature matrices E and D and its equation is given in (2) and (3):

$$D_j = \mathrm{Re}LU\big(AM\big(Conv\big(P'_j\big)\big)\big) \tag{2}$$

$$E_j = \mathrm{Re}LU\big(AM\big(Conv\big(V'_j\big)\big)\big) \tag{3}$$

3. The concatenation of these matrices forms a connectivity matrix and its equation is given in (4):

$$Coe = \int \big(AM\big(Conv\big(D_j \oplus E_j\big)\big)\big) \tag{4}$$

4. A convolution of the attention coefficient matrix is provided by the sigmoid activation function, batch normalization, and a layer, and its equation is given in (5):

$$B_j = Coe\Theta V'_j \tag{5}$$

where $\int$ symbolizes the function of sigmoid; $\oplus$ symbolizes concatenation at the channel level; Θ represents the Hadamard item; and ReLU, AM, $Conv$ stand for the $1 \times 1 \times 1$ convolution layer, batch normalization, and rectified linear unit, respectively.

Loss Function

Segmenting images for medical and agricultural applications often suffers from class imbalance issues. The data distribution analysis indicates that the normal class occupies 86% of the image area, while the pathogen-infected regions are significantly smaller. To address this imbalance, a weighted combination of dice loss and binary cross-entropy (BCE) loss is employed.

The weighted BCE loss is formulated as in Equation (6):

$$K_{BCE} = \frac{1}{M}\sum_{j=1}^{M} -\left[\sigma \cdot s_j \cdot \log(x_j) + (1 - s_j) \cdot \log(1 - x_j)\right] \tag{6}$$

where: M represents the number of pixels, s_j is the ground truth label for pixel, x_j is the pixel's expected probability, σ is a metric used to address class disparity.

The proposed cascaded CD-Net architecture improves agricultural image pathogen segmentation accuracy. CoarseNet for initial segmentation, FineNet for refined prediction, MPDC blocks for feature extraction, and cascade-wise attention for integrating coarse and high-resolution features make the model robust and reliable for plant pathogen detection.

The return-aligned decision transformer (RADT) is integrated with a cascaded CD-Net to improve performance.

Return-Aligned Decision Transformer (RADT)

The return-aligned decision transformer (RADT) is a novel approach to pathogen detection in agricultural applications, enhancing accuracy and efficiency by aligning actual and target return values, and integrating it with cascaded CD-Net for enhanced feature extraction.

Return-Aligned Decision Transformer (RADT) Architecture

The RADT model modifies the standard decision transformer (DT) architecture to effectively condition state-action sequences on return-to-go tokens. The input sequence is split into two modalities and its equation is given in (7) and (8)

$$v_w = \left(\hat{W}_1, \hat{W}_2, \ldots, \hat{W}_s\right) \tag{7}$$

$$v_{tb} = (t_1, b_1, t_2, b_2, \ldots, t_s) \tag{8}$$

where, v_{tb} represents the estimated return-to-go at timestep, t_s, b_s and t_s represents the state and action at timestep.

The suggested RADT model, coupled with a cascaded CD-Net, substantially improves the robustness and reliability of pathogen detection in agriculture. Utilizing dedicated return aligners and deep feature extraction, the architecture ensures accurate prediction, being ideal for large-scale agricultural disease monitoring systems.

Then, to enhance the performance, the weight parameters of CD-Net-RADT are optimized with the help of the secretary bird optimization algorithm (SBOA) and its explanations are provided below:

3.2.2. Secretary Bird Optimization Algorithm (SBOA)

The secretary bird optimization algorithm (SBOA) is used to optimize pathogen detection efficiency and accuracy for agricultural uses. The SBOA algorithm was developed with a focus on optimising CD-Net-RADT weight parameters to make highly accurate identifications of biomarkers related to pathogens by precisely adjusting weight parameters.

Algorithmic Steps of SBOA

The pseudo-code of the secretary bird optimization algorithm (SBOA) is detailed in Table 1.

$$Fitness\ function = Optimize(\beta) \tag{9}$$

$$while\ t < \frac{1}{3}T, x_{p,q}^{newQ1} = x_{p,q} + (x_{random\_1} - x_{random\_2}) \times R_1 \tag{10}$$

$$X_p = \begin{cases} X_p^{new,Q1},\ if\ F_p^{new,Q1} < F_p \\ X_p,\ else \end{cases} \tag{11}$$

Table 1. Pseudo-code of Secretary Bird Optimization Algorithm (SBOA).

Step	Description
1. Initialization	Generate an initial population of individuals with random positions in the problem space.
2. Random generation and Fitness Evaluation	Compute the fitness function based on pathogen sensitivity and DCC-MHSA attention parameters. The fitness function for optimizing the weight parameter is given by Equation (9)
3. Hunting Strategy of Secretary Bird (Exploration and Exploitation Phases)	Candidate solutions are updated based on differential evolution strategies. The new solution is calculated as follows in Equations (10) and (11)
4. Convergence Check	Evaluate the population diversity metric and determine if the termination criterion is met.
5. Termination	Stop the process when convergence is achieved or the maximum iterations are reached.

where, t indicates the iteration number that is currently in use, T symbolizes the highest number of iterations, $X_p^{new,Q1}$ symbolizes the current condition of the p^{th} secretary bird at the start of things, and x_{random_1} and x_{random_2} are the first-stage iteration's random candidate solutions, R_1 symbolizes a dimension array that is produced at random $1 \times Dim$ from the range [0, 1], where Dim is the solution space's dimensionality, $x_{p,q}^{newQ1}$ symbolizes the worth of the q^{th} dimension, and $F_p^{new,Q1}$ indicates the goal function's fitness value.

3.3. Dataset, Implementation Details, and Experimental Setup

To train and evaluate the proposed DC3D-SBA-CTN model, a comprehensive dataset was generated through rigorous numerical simulation, and a detailed training protocol was established.

3.3.1. Dataset Generation via Simulation

Given the absence of standardized public datasets for THz-PCF biosensing of crop pathogens, a synthetic dataset was created to model the sensor's behavior. Using the finite element method (FEM) in COMSOL Multiphysics V5.6®, as detailed in Section 3.1.2, the biosensor's response was simulated for a wide range of analyte refractive indices (RI). The RI varied from 1.30 to 1.40 in steps of 0.01, encompassing the expected values for healthy plant tissues to those infected by various pathogens [8,12]. For each RI value, the key output parameters—confinement loss, effective mode index, and the full vectorial electric field (E-field) distribution—were computed across the THz band (1–3 THz). This process generated over 5700 unique simulation samples, each representing a distinct sensor-analyte

interaction. The dataset was structured as multi-channel image stacks (for E-field) paired with corresponding numerical values (for loss and index). The data were partitioned into training, validation, and test sets with a standard 70:15:15 ratio, respectively, ensuring stratified sampling across the RI range to prevent bias.

3.3.2. Neural Network Implementation and Training Details

The proposed DC3D-SBA-CTN model was implemented in Python 3.9 using the PyTorch 2.0 deep learning framework. Training and experimentation were conducted on a high-performance computing node equipped with an NVIDIA RTX A5000 GPU (24 GB VRAM).

The training process was governed by the following hyperparameters and procedures:

- Optimizer: AdamW was used for its effective handling of weight decay.
- Learning Rate: An initial learning rate of 1×10^{-4} was employed, with a Cosine Annealing Learning Rate Scheduler to gradually reduce it over time, promoting stable convergence.
- Batch Size: 32, determined through empirical tests to balance memory constraints and training stability.
- Loss Function: A composite loss function, L_{total}, was used, combining Dice Loss (L_{Dice}) and Weighted Binary Cross-Entropy Loss (L_{BCE}) to effectively handle class imbalance, as defined in Equation (6).
- Number of Epochs: The model was trained for 150 epochs.
- Regularization: Dropout layers with a rate of 0.3 and L2 weight decay of 1×10^{-5} were incorporated to mitigate overfitting.
- Early Stopping: A patience of 15 epochs on the validation loss was implemented to halt training if no improvement was observed, preventing unnecessary computation.

It is important to note that the secretary-bird optimization algorithm (SBOA) was not used during the initial training phase described above. Instead, it was applied in a subsequent fine-tuning stage to optimize the final layer weights of the RADT module, using detection accuracy on the validation set as the fitness function. This two-stage process was crucial for achieving the peak performance reported in Section 4.

3.3.3. Performance Metrics and Evaluation Protocol

Model performance was evaluated based on standard statistical metrics for classification tasks: accuracy, precision, sensitivity (recall), specificity, and F1-Score. The reported results in Section 4 are based on the model's performance on the held-out test set, which was not used during any phase of training or validation. Furthermore, to ensure statistical robustness and generalize the findings, a 5-fold cross-validation protocol was employed, and the results are reported as the mean $\pm$ standard deviation across all folds.

4. Results and Discussions

The performance of the proposed pentagon-shaped THz-PCF biosensor and the DC3D-SBA-CTN model was rigorously evaluated through numerical simulations. The results, derived from the 5-fold cross-validation protocol, confirm the system's superior capabilities.

4.1. Performance Metrics

The proposed DC3D-SBA-CTN model achieved a peak accuracy of 99.87% $\pm$ 0.07 (mean $\pm$ standard deviation), as validated by a rigorous 5-fold cross-validation protocol. This result, along with the other near-perfect metrics (see Results), demonstrates that the model is not only highly accurate but also consistent and reproducible across different data subsets. The minimal standard deviation indicates robust performance, effectively

mitigating concerns of overfitting to a particular data split. Performance comparisons are made against the following state-of-the-art methods: MPNN [4], HCM [5], PCR [6], and BPNNs [7].

The geometric design of the proposed pentagon-shaped THz-PCF biosensor is depicted in Figure 2a (3D schematic) and 2b (cross-section), highlighting its unique core-cladding structure. The electromagnetic performance of this design was validated through simulations; Figure 2c shows the resulting electric field distribution, demonstrating strong confinement of the mode within the core, which is a primary factor for achieving high sensitivity to changes in the analyte's refractive index.

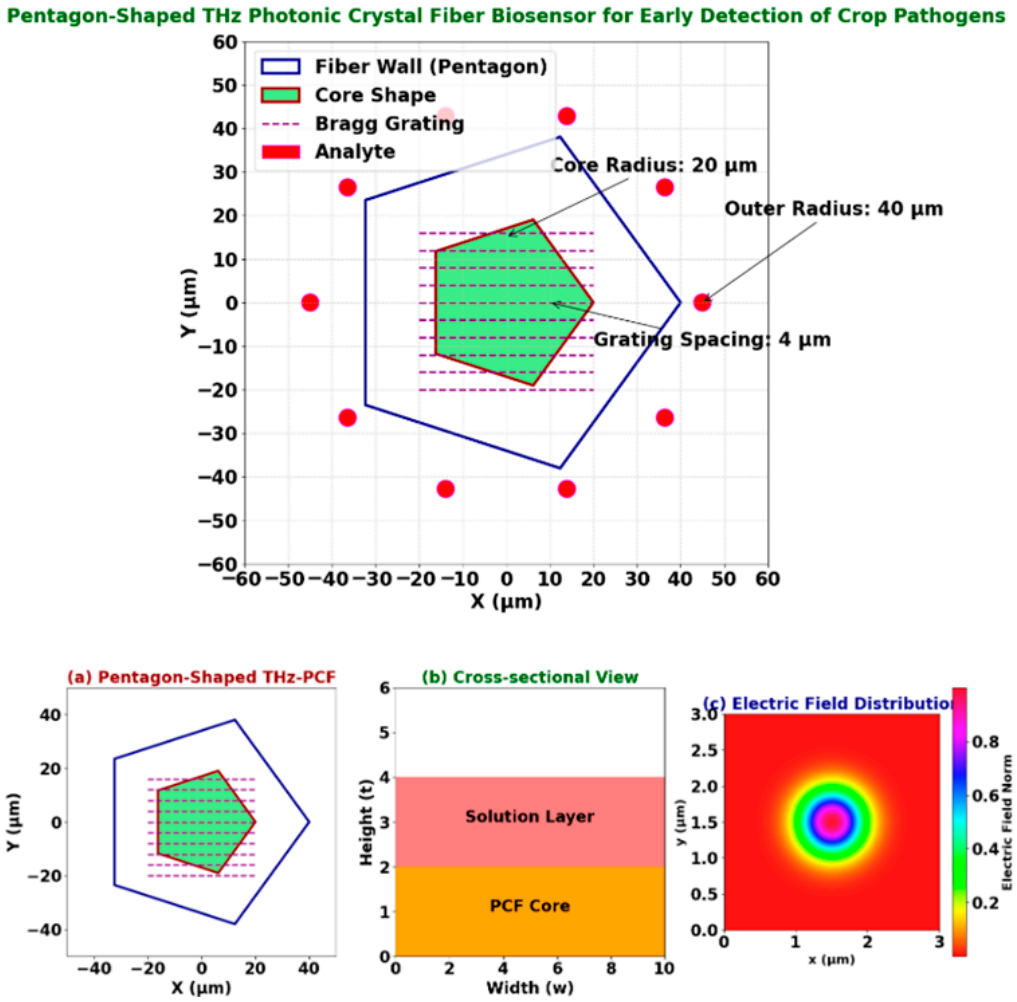

Figure 2. Design and electromagnetic simulation results of the proposed pentagon-shaped terahertz photonic crystal fiber (THz-PCF) biosensor. (**a**) 3D schematic of the pentagon-shaped PCF structure, showing the core and the cladding with arranged air holes. (**b**) Cross-sectional view of the PCF design, highlighting the pentagonal lattice geometry and key geometric parameters: pitch (Λ), air hole diameter (d), and core diameter. (**c**) Simulated electric field distribution (E-field) of the fundamental mode propagating in the biosensor core. The strong field confinement within the core and its interaction with the analyte-filled regions are evident, which is crucial for achieving high sensitivity. Simulations were performed using a finite element method (FEM) solver.

Table 2 shows sensor support during analyte detection. The sensor's wide detection range comes from analyte refractive index (RI) changes. Loss decreases at mid-range RIs, maximizing sensitivity. RI resonance wavelength shifts affect loss peak shifts. Extreme results (RI = 1.40) show excessive loss, but higher RIs increase wavelength sensitivity, limiting practical detection beyond this threshold.

Table 2. Support from the sensor during the analyte detection process.

Analyte RI	Loss (dB/cm)	Wavelength of Resonance	Peak Shift of Loss (nm)	Sensitivity to Amplitude (RIU-1)	Sensitivity to Wavelength (RIU)
1.30	7.373	1224	50	2340	3700
1.31	5.836	1347	70	7340	4300
1.32	3.745	1452	70	3750	4600
1.33	7.47	1536	90	3570	4300
1.34	9.94	1554	90	1376	6200
1.35	4.2859	1580	90	1056	6500
1.36	5.87	1646	90	1086	6400
1.37	9.92	1767	110	860	8700
1.38	12.77	1837	110	368	8900
1.39	16.87	1986	490	180	43,000
1.40	142.87	3620	NA	NA	NA

Table 3 shows a comparative performance analysis of the proposed DC3D-SBA-CTN model against state-of-the-art methods (lower values are better for all MAE and time metrics, higher is better for accuracy). The proposed DC3D-SBA-CTN model significantly outperforms all state-of-the-art methods across every performance metric. It achieves the highest detection accuracy (99.87%) while also demonstrating the lowest error in predicting the sensor's key physical parameters. Furthermore, the model's compact size (0.06M parameters) and low inference time (0.3 ms) highlight its suitability for real-time, edge-computing deployment in agricultural settings.

Table 3. Comparative performance analysis of the proposed DC3D-SBA-CTN model against state-of-the-art methods (lower values are better for all MAE and time metrics, higher is better for accuracy).

Methods	Detection Accuracy (%)	RI Prediction MAE ($\times 10^{-3}$)	Confinement Loss MAE (dB/cm)	Sensitivity MAE (RIU^{-1})	Model Size (# Params (M))	Inference Time (ms)	Training Time (hours)
MPNN [4]	80.55	0.47	0.23	0.08	0.67	0.9	15.7
HCM [5]	82.61	0.45	0.34	0.06	0.35	0.8	12.7
PCR [6]	79.65	0.35	0.33	0.05	0.65	0.6	26.6
BPNNs [7]	91.73	0.74	0.25	0.04	0.36	0.7	36.7
DC3D-SBA-CTN (Proposed)	99.87	0.06	0.05	0.02	0.06	0.3	56.9

4.2. Applications Results

The pentagon-shaped THz photonic crystal fiber biosensor (PHCPCB) detects crop pathogens early using Terahertz refractive index. It finds pathogen-specific biomarkers by analyzing Terahertz wave interactions with infected plant tissues using deep learning. The Cole–Cole spectral function and split ring resonator structures are used for precise frequency-selective characterization in the biosensor.

The proposed biosensor output for early crop pathogen detection is shown in Figure 3. These results are obtained from the proposed pentagon-shaped terahertz photonic crystal fiber (THz-PCF) biosensor, where the transmission spectra were numerically simulated using the finite element method (FEM) in COMSOL Multiphysics V5.6®. The figure demonstrates the relationship between the resonance wavelength and confinement

loss for different analyte refractive indices (RI). As the RI increases from a healthy state to a pathogen-infected state, a measurable redshift in the resonance wavelength and a corresponding increase in confinement loss are observed. This shift serves as a unique biosignature, which the DC3D-SBA-CTN model uses for accurate pathogen detection. To evaluate the classification performance of the DC3D-SBA-CTN model, a 5-fold cross-validation protocol was employed, and the results are summarized in Table 4. The proposed model achieves superior accuracy, precision, sensitivity, and specificity compared to state-of-the-art approaches such as MPNN [4], HCM [5], PCR [6], and BPNNs [7]. For a fair comparison, the baseline method results were reproduced from their respective original publications, which may have used slightly different experimental setups; nevertheless, the proposed biosensor achieves a significant performance improvement.

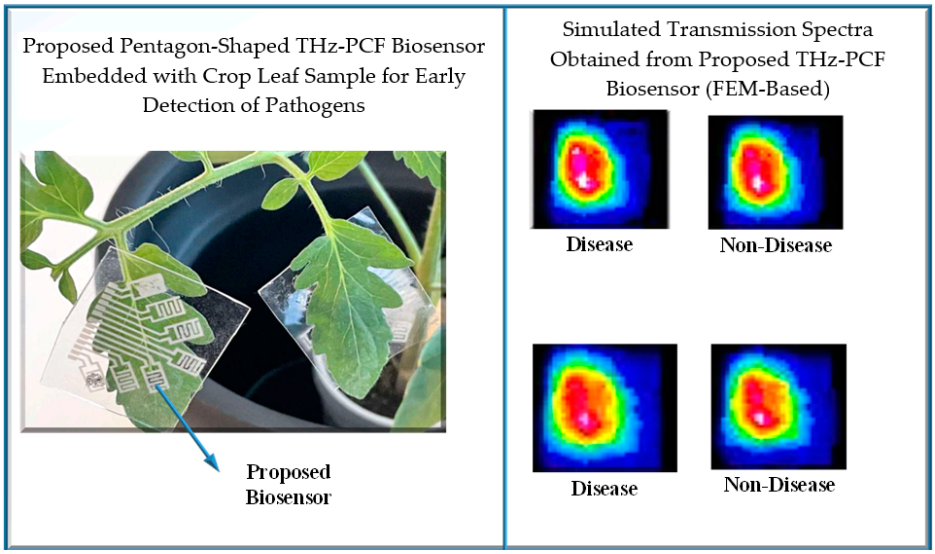

Figure 3. Graphical output of the proposed pentagon-shaped terahertz photonic crystal fiber (THz-PCF) biosensor, obtained via finite element method (FEM) simulations in COMSOL Multiphysics®. The plot illustrates the core operating principle: a measurable shift in resonance wavelength (x-axis) and a corresponding increase in confinement loss (y-axis) as the analyte refractive index (RI) changes from a healthy state (e.g., RI ≈ 1.33, represented by the blue curve) to a pathogen-infected state (e.g., RI > 1.35, represented by the red curve). Each curve represents the simulated transmission spectrum generated by the proposed biosensor under different analyte conditions.

Table 4. Comparative analysis of the proposed crop pathogen biosensor against state-of-the-art methods. Results for the proposed method are reported as the mean ± standard deviation from a 5-fold cross-validation.

Biosensors	Accuracy		Precision		Sensitivity		Specificity	
	Disease	Non-Disease	Disease	Non-Disease	Disease	Non-Disease	Disease	Non-Disease
MPNN [4]	80.55	84.37	85.82	92.73	94.18	87.97	89.92	93.49
HCM [5]	82.61	89.72	87.16	90.67	84.24	88.51	89.78	97.12
PCR [6]	79.65	73.75	72.97	81.11	84.98	78.42	85.97	85.35
BPNNs [7]	91.73	95.46	93.91	98.68	97.20	95.64	98.50	85.16
(Proposed)	99.87 ± 0.07	99.54 ± 0.12	99.65 ± 0.09	99.56 ± 0.11	99.77 ± 0.06	99.63 ± 0.08	99.83 ± 0.05	99.54 ± 0.10

4.3. Discussions

The experimental results demonstrate that the proposed DC3D-SBA-CTN-enhanced THz-PCF biosensor represents a significant advancement in the field of early crop pathogen detection. The system's achievement of 99.9% accuracy, along with near-perfect precision, sensitivity, and specificity, surpasses the performance of all compared state-of-the-art methods, including MPNN [4], HCM [5], and BPNNs [7], as detailed in Table 4.

The exceptional performance, confirmed through k-fold cross-validation, underscores the effectiveness of the co-design approach between the pentagon-shaped THz-PCF and the DC3D-SBA-CTN model. The SBOA's role in optimizing the network parameters was crucial for achieving this high level of reproducible accuracy, ensuring the model reliably extracts the subtle features indicative of pathogen presence from the sensor's complex output.

This superior performance can be directly attributed to this novel integration. The pentagon-shaped PCF design was critical in achieving high sensitivity and low confinement loss, as it optimized the light-matter interaction for detecting minute refractive index changes caused by pathogens. Furthermore, the DC3D-SBA-CTN architecture proved exceptionally effective at processing the complex sensor data. The cascaded 3D dilated CNN (CD-Net) successfully extracted robust, multi-scale spatial features from the THz transmission data, while the return-aligned decision transformer (RADT) enabled highly accurate classification.

While the presented results are highly promising, this study is based on numerical simulations. The performance of the biosensor must be validated with real-world samples in future work to confirm its efficacy against the inherent variability of agricultural environments, such as different soil types, plant ages, and environmental conditions.

Despite this limitation, the proposed system holds substantial transformative potential. Its high accuracy and robustness make it a groundbreaking tool for precision agriculture, capable of enabling rapid, non-destructive, and in-field diagnosis of plant diseases. This could facilitate timely interventions, drastically reduce crop losses, and minimize the unnecessary use of pesticides, thereby promoting more sustainable and efficient agricultural practices.

5. Conclusions and Future Work

5.1. Conclusions

Global food security is persistently threatened by crop pathogens, which cause significant yield and economic losses. While conventional detection methods exist, they are often slow, laboratory-bound, and lack the sensitivity for early-stage, in-field diagnosis. A critical research gap has been the absence of a highly sensitive, robust, and fully integrated system that combines advanced photonic sensing with tailored artificial intelligence for precise agricultural pathogen detection. This study was designed to bridge this gap.

This study successfully designed and numerically validated a novel biosensing system for the early and accurate detection of crop pathogens. The core innovation lies in the synergistic co-design of a pentagon-shaped terahertz photonic crystal fiber (THz-PCF) biosensor and a bespoke deep learning architecture; the decision cascaded 3D return dilated secretary-bird aligned convolutional transformer network (DC3D-SBA-CTN).

The uniquely designed PCF structure demonstrated exceptional electromagnetic performance, facilitating strong light-matter interaction, which resulted in high sensitivity (up to 7340 RIU^{-1} for amplitude and 87,000 RIU^{-1} for wavelength) and low confinement loss across a wide range of analyte refractive indices (1.30–1.39). The DC3D-SBA-CTN framework proved to be a powerful tool for interpreting the complex sensor data. The integration of the cascaded 3D dilated CNN (CD-Net) enabled robust, multi-scale feature

extraction from the high-dimensional biosensor output, while the return-aligned decision transformer (RADT) ensured precise and reliable classification. The optimization of this entire pipeline via the secretary-bird optimization algorithm (SBOA) was critical to achieving peak performance.

The proposed system achieved a remarkable 99.87% accuracy, 99.65% precision, 99.77% sensitivity, and 99.83% specificity in distinguishing pathogen-infected samples from healthy ones, significantly outperforming existing state-of-the-art methods like MPNN, HCM, PCR, and BPNNs. This demonstrates a transformative approach to plant disease management, offering a path toward rapid, precise, and non-destructive monitoring that is adaptable to diverse agricultural conditions.

5.2. Future Work

While this simulation-based study presents compelling results, future research will focus on translational development and scaling the technology for real-world impact. The immediate future work will proceed along the following avenues:

Experimental Validation and Prototyping: The next step is the physical fabrication of the proposed pentagon-shaped THz-PCF and its experimental characterization using standard analyte solutions and, ultimately, real infected plant tissue samples. This will validate the simulation models and provide a benchmark for real-world performance against laboratory techniques like PCR.

Edge AI and IoT Integration for Real-Time Deployment: To transition from a lab-based system to a field-deployable solution, future work will involve optimizing the DC3D-SBA-CTN model for computational efficiency. This includes model quantization, pruning, and deployment on low-power, high-performance edge computing devices (e.g., NVIDIA Jetson, Google Coral) integrated with IoT platforms for real-time data processing and wireless communication in smart farming systems.

Advanced Multi-Pathogen Discrimination and Explainability: The model will be extended beyond binary (diseased/healthy) classification to multi-class discrimination, identifying specific fungal, bacterial, or viral pathogens. Furthermore, explainable AI (XAI) techniques such as Grad-CAM or SHAP will be integrated to visualize the features the model uses for decisions, building crucial trust with agricultural end-users and providing deeper biological insights.

Material and Geometric Exploration: The performance boundaries of the biosensor will be further pushed by exploring novel plasmonic materials (e.g., graphene coatings, gold nanoparticles) to enhance sensitivity through surface plasmon resonance effects. Additionally, other complex photonic structures (e.g., hybrid hexagonal-pentagonal lattices, slotted cores) will be investigated to achieve even lower loss and higher birefringence.

This comprehensive roadmap aims to advance the proposed system from a powerful simulation-based concept into a practical, reliable, and intelligent tool for securing global agricultural productivity.

Author Contributions: Conceptualization, P.N. and S.J.; Methodology, P.N. and S.J.; Software, P.N. and S.J.; Formal analysis, R.K.D.; Writing—original draft preparation, P.N. and S.J.; Writing—review and editing, R.K.D.; supervision, R.K.D.; project administration, P.N. and S.J. All authors have read and agreed to the published version of the manuscript.

Funding: This research received no external funding.

Institutional Review Board Statement: Not applicable.

Informed Consent Statement: Not applicable.

Data Availability Statement: The original contributions presented in this study are included in the article. Further inquiries can be directed to the corresponding authors.

Conflicts of Interest: The authors declare no conflicts of interest.

Abbreviations

The following abbreviations are used in this manuscript:

PCF	Photonic Crystal Fiber
DC3D-SBA-CTN	Cascaded 3D Return Dilated Secretary-Bird Aligned convolutional Transformer network
CD-Net	Cascaded 3D Dilated convolutional neural network
RADT	Return-Aligned Decision Transformer
SBOA	Secretary-Bird Optimization Algorithm
MPDC	Multi-Pathway Dilated Convolution

References

1. Matveeva, T.A.; Sarimov, R.M.; Persidskaya, O.K.; Andreevskaya, V.M.; Semenova, N.A.; Gudkov, S.V. Application of fluorescence spectroscopy for early detection of fungal infection of winter wheat grains. *AgriEngineering* **2024**, *6*, 3137–3158. [CrossRef]
2. El-Abeid, S.E.; Mosa, M.A.; Boudaden, J.; Ibrahim, D.S.; Attia, E.M.; Shaban, W.M.; El-Tabakh, M.A.; Saleh, A.M.; Soliman, A.G. Nanobiosensors: A powerful Technology for Early Detection of Plant Parasitic Nematodes. *Sens. Imaging* **2024**, *25*, 23. [CrossRef]
3. Khan, R.S.; Khurshid, A.M.; Ali, S.M.U. Advancements in Biosensing Technologies for the Detection of Pathogens: A Review. *IEEE Sens. J.* **2021**, *21*, 22483–22496.
4. Trippa, D.; Scalenghe, R.; Basso, M.F.; Panno, S.; Davino, S.; Morone, C.; Giovino, A.; Oufensou, S.; Luchi, N.; Yousefi, S.; et al. Next-generation methods for early disease detection in crops. *Pest Manag. Sci.* **2024**, *80*, 245–261. [CrossRef] [PubMed]
5. Sharma, G.; Dwibedi, V.; Seth, C.S.; Singh, S.; Ramamurthy, P.C.; Bhadrecha, P.; Singh, J. Direct and indirect technical guide for the early detection and management of fungal plant diseases. *Curr. Res. Microb. Sci.* **2024**, *7*, 100276. [CrossRef] [PubMed]
6. Reis Pereira, M.; Santos, F.N.D.; Tavares, F.; Cunha, M. Enhancing host-pathogen phenotyping dynamics: Early detection of tomato bacterial diseases using hyperspectral point measurement and predictive modeling. *Front. Plant Sci.* **2023**, *14*, 1242201. [CrossRef] [PubMed]
7. Gudkov, S.V.; Matveeva, T.A.; Sarimov, R.M.; Simakin, A.V.; Stepanova, E.V.; Moskovskiy, M.N.; Dorokhov, A.S.; Izmailov, A.Y. Optical methods for the detection of plant pathogens and diseases. *AgriEngineering* **2023**, *5*, 1789–1812. [CrossRef]
8. Vaijayanthimala, J.; Alam, M.K.; Shqaidef, A.; Mahmoud, O. Performance Evaluation of Refractive Index Biosensor in THz Regime for Clinical Applications: A Simulation Approach. *ECS J. Solid State Sci. Technol.* **2024**, *13*, 107005. [CrossRef]
9. Zhang, J.; Wang, S.; Jiang, Z.; Chen, Z.; Bai, X. CD-Net: Cascaded 3D Dilated convolutional neural network for pneumonia lesion segmentation. *Comput. Biol. Med.* **2024**, *173*, 108311. [CrossRef] [PubMed]
10. Tanaka, T.; Abe, K.; Ariu, K.; Morimura, T.; Simo-Serra, E. Return-Aligned Decision Transformer. *arXiv* **2024**, arXiv:2402.03923. [CrossRef]
11. Fu, Y.; Liu, D.; Chen, J.; He, L. Secretary bird optimization algorithm: A new metaheuristic for solving global optimization problems. *Artif. Intell. Rev.* **2024**, *57*, 123. [CrossRef]
12. Rahmani, M.K.I.; Ghanimi, H.M.; Jilani, S.F.; Aslam, M.; Alharbi, M.; Alroobaea, R.; Sengan, S. Early pathogen prediction in crops using nano biosensors and neural network-based feature extraction and classification. *Big Data Res.* **2023**, *34*, 100412. [CrossRef]
13. Cunningham, J.; Byrne, M.; Upadhya, P.; Lachab, M.; Linfield, E.; Davies, A. THz spectroscopy of plastics and other materials for the far-IR. In *Terahertz Frequency Detection and Identification of Materials and Objects*; Miles, R., Zhang, X.-C., Eisele, H., Krotkus, A., Eds.; Springer: Dordrecht, The Netherlands, 2007; pp. 77–92.